Journal of Materials Chemistry C

PAPER

View Article Online
View Journal | View Issue

Cite this: J. Mater. Chem. C, 2014, 2, 7785

Nonlinear optical chromophores containing a novel pyrrole-based bridge: optimization of electro-optic activity and thermal stability by modifying the bridge†

Fenggang Liu,[ab] Haoran Wang,[ab] Yuhui Yang,[ab] Huajun Xu,[ab] Maolin Zhang,[ab] Airui Zhang,[ab] Shuhui Bo,*[a] Zhen Zhen,[a] Xinhou Liu[a] and Ling Qiu*[a]

Received 2nd May 2014
Accepted 16th July 2014

DOI: 10.1039/c4tc00900b

www.rsc.org/MaterialsC

Three novel second order nonlinear optical chromophores based on julolidinyl donors and tricyanovinyldihydrofuran (TCF) acceptors linked together *via* modified pyrrole π-conjugation (chromophores A and B) or thiophene moieties (chromophore C) as the bridges have been synthesized and systematically characterized. In particular, the pyrrole moiety bridge has been modified with the electron withdrawing group (–Br, $-NO_2$) substituted benzene ring. The introduction of side phenyl groups to chromophores A and B can increase the thermal and chemical stability and reduce dipole–dipole interactions so as to translate their hyperpolarizability (β) values into bulk EO performance more effectively than chromophore C. Moreover, DFT calculations suggested that the additional electron withdrawing groups in chromophores A and B could increase the β value compared to that of chromophore D without substituted phenyl groups, and they showed different influences on the solvatochromic behavior, thermal stability, and electro-optic activity of the chromophores. EO responses (r_{33} values) of guest–host polymers containing pyrrole-bridged chromophores were reported. Incorporation of chromophores A and B into APC provided large electro-optic coefficients of 86 and 128 pm V^{-1} at 1310 nm with a high loading of 30 wt%. Film-C/APC containing 25 wt% of chromophore C provides an EO coefficient of 98 pm V^{-1}.

1. Introduction

In recent years, organic electro-optic (OEO) materials have attracted great attention owing to their potential applications in optical switches, optical sensors, information processors, telecommunications, *etc.*[1–3] Compared with inorganic materials, OEO materials have potential advantages such as lower cost, ease of processing, larger EO coefficients and so on.[4–6] To meet the stringent requirements for the use of devices, OEO materials should be developed through the rational design of nonlinear optical (NLO) chromophores to optimize their first hyperpolarizability (β), and effectively translate these large β values into bulk EO activities together with improvement of other auxiliary properties like high thermal and chemical stability.[7]

The second-order NLO chromophores are based on a push–pull system, which consists of an electron-donating group (donor) and an electron-withdrawing group (acceptor) coupled through a π-conjugated bridge.[8,9] Among the many types of NLO chromophores developed so far, strong electron donor and acceptor groups connected by chemically and thermally stable conjugated π-bridges have been widely employed.[10] Until now, NLO chromophores containing thiophene,[11,12] locked phenyltetraene,[7] azo[13] and phenyltetraene-based[14] bridges have been reported. Among which thiophene and phenyltetraene bridges were widely used. Further modification was widely studied to achieve excellent and better performance.[14,15] However, the pyrrole-based bridge,[16] the analogue of furan and thiophene moieties, has seldom been noticed, especially for chromophores with a strong donor and a strong acceptor possibly due to its unstability. In fact, to the best of the authors' knowledge, few studies have reported on the macroscopic EO response (r_{33} value) of poled films containing pyrrole-bridged chromophores. Practical applications of second-order NLO materials require thermally and chemically robust materials with a high electro-optic (EO) coefficient (r_{33}) value.

The above points prompted us to design and synthesize a series of pyrrole-bridged NLO chromophores with enhanced stability. Moreover, the β values of these chromophores can be effectively translated into high EO activities in poled polymers

[a]Key Laboratory of Photochemical Conversion and Optoelectronic Materials, Technical Institute of Physics and Chemistry, Chinese Academy of Sciences, Beijing 100190, PR China. E-mail: boshuhui@mail.ipc.ac.cn; qiuling@mail.ipc.ac.cn; Fax: +86-01-2543529; Tel: +86-01-82543529

[b]University of Chinese Academy of Sciences, Beijing 100043, PR China

† Electronic supplementary information (ESI) available. See DOI: 10.1039/c4tc00900b

by suitable shape engineering. Modifications of the pyrrole-bridge have been explored for high electro-optic coefficients along with improved chemical and thermal stability to withstand high temperatures encountered in electric field poling and subsequent processing of chromophore/polymer materials. So that it can be applied to electro-optic materials.

We used a strong julolidinyl-based donor[17,18] and tricyanovinyldihydrofuran (TCF) acceptor to construct our chromophores. In our syntheses, we found that when used as a bridge, the abundant electron density of the pyrrole makes it unstable. So, the labile nitrogen proton was replaced with aromatic blocks to improve the stability. Moreover, a new method was proposed to introduce some electron-withdrawing units, which acted as additional electron acceptors, to form special types of organic chromophores. The additional electron acceptors (–Br, $–NO_2$) were substituted on the benzene ring so that the properties (like electron density) of the chromophore can be changed. The roles of different auxiliary acceptor groups connected to the conjugated spacers of push–pull chromophores have been investigated and evaluated by theoretical methods. These introduced acceptor groups could not only increase the β values, but also reduce dipole–dipole interactions of these chromophores to improve the EO activity.

In this study, we had designed and synthesized chromophores A and B based on modified pyrrole bridges. Chromophore C containing a thiophene bridge had been synthesized for comparison (Chart 1). The UV-Vis, solvatochromic, redox properties, density functional theory (DFT) quantum mechanical calculations, thermal stabilities and EO activities of these chromophores were systematically studied and compared to illustrate the influences of the modified bridges on rational NLO chromophore designs. Previous studies showed that the DFT method is considered reliable in predicting trends in hyperpolarizability,[19] and have been shown to predict experimental trends accurately.[20] Chromophore D containing unmodified pyrrole bridge had not been synthesized due to its chemical and thermal instability. However, the use of theoretical methods enables us to study the effects of structural modifications on optimization of chromophore hyperpolarizability in this series of molecules.

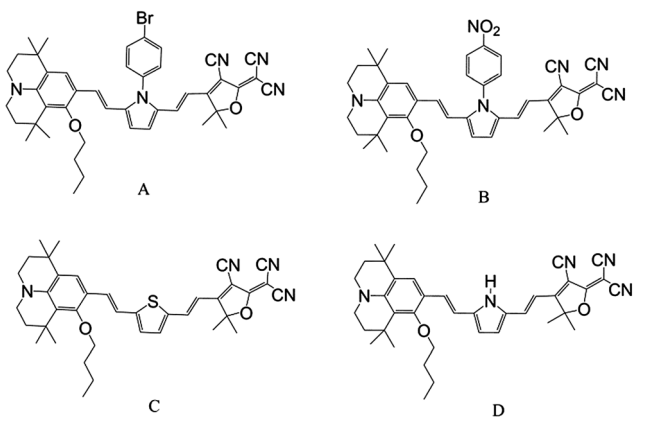

Chart 1 Chemical structures for chromophores A, B, C, and D.

2. Results and discussion

2.1 Synthesis and characterization of chromophores

Scheme 1 shows the synthetic approach to the new chromophores A, B, and C. Starting from the amine donor aldehyde intermediate compound **3**, chromophores A, B, and C were synthesized in good overall yields through simple four main step reactions. The free hydroxyl group on the donors was protected by the alkyl group to improve the solubility through Williamson ether synthesis, after introduction of the bridge by Wittig condensation; compounds **5a–c** were prepared in a high yield. Treatment of compounds **5a** and **b** with $POCl_3$ and DMF gave aldehydes **6a** and **b**. Treatment of compound **5c** with *n*-BuLi and DMF gave an aldehyde **6c**. And the final condensations with the TCF acceptor give chromophores A, B, and C all as green solids. All of the chromophores were fully characterized by ^{1}H-NMR, ^{13}C-NMR, elemental analysis and mass spectroscopy. These chromophores possess good solubility in common organic solvents, such as dichloromethane, chloromethane and acetone.

2.2 Thermal stability

The NLO chromophores must be thermally stable in order to withstand the poling process and subsequent processing for use. The thermal stability of the chromophores was investigated using thermogravimetric analysis (TGA) and differential scanning calorimetry (DSC) as shown in Fig. 1. Chromophores B and C appeared as highly crystalline compounds with a melting point at 196 °C and 198 °C, respectively, while chromophore A was obtained as an amorphous solid showing a glass transition

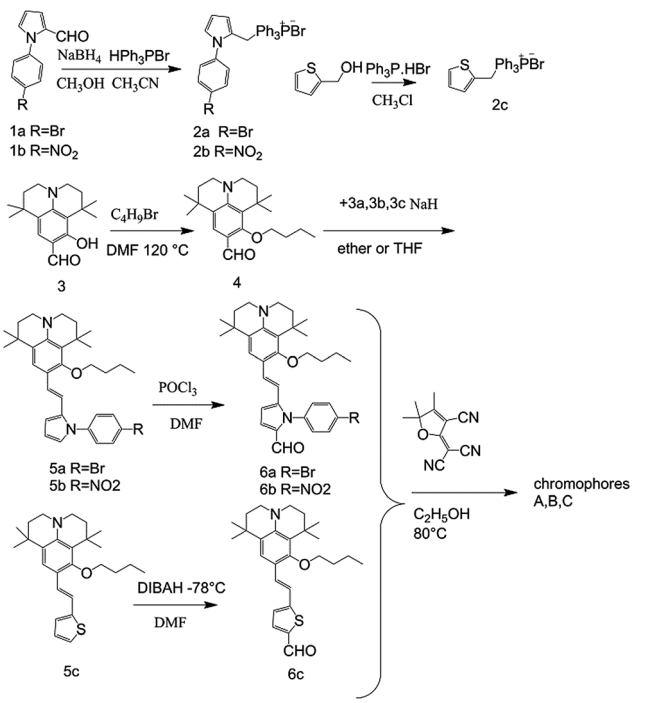

Scheme 1 Chemical structures and synthetic routes to chromophores A, B, and C.

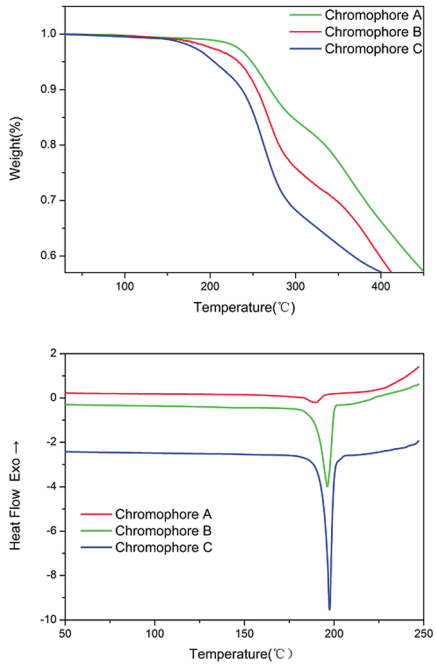

Fig. 1 TGA and DSC curves of chromophores A–C with a heating rate of 10 °C min^{-1} in a nitrogen atmosphere.

temperature (T_g) at 190 °C. All the chromophores exhibited good thermal stabilities with the decomposition temperatures (T_d) higher than 200 °C (202–251 °C). Chromophore A had the maximum decomposition temperature (T_d = 251 °C). Chromophores A and B had higher decomposition temperature than that of chromophore C with a thiophene bridge (T_d = 202 °C). The enhanced thermal stability of chromophores A and B over chromophore C is due to the introduction of a benzene ring into π-bridge pyrrole. While chromophores A and B had a similar pyrrole bridge, they show different decomposition temperatures of 251 °C and 236 °C, respectively. This may be due to the different properties of modified groups (–Br, $–NO_2$). The data indicate that the modified groups can influence the thermal stabilities of chromophores, and thus we can modify the pyrrole bridge to improve the thermal properties.

2.3 Optical properties

To explore the different charge-transfer (CT) absorption properties of each chromophore, UV-Vis absorption spectra of three chromophores were recorded in a series of solvents with different dielectric constants and in films, as shown in Fig. 2. The spectral data are summarized in Table 1. It may be seen from Fig. 2 that chromophores A, B and C show the maximum absorption (λ_{max}) from 723 nm to 728 nm in chloroform. Compared to chromophore C, chromophores A and B were slightly blue-shifted ($\Delta\lambda$ = 5 nm, $\Delta\lambda$ = 3 nm), and the two compounds containing the pyrrole bridge exhibited a similar charge-transfer band shape.

Besides, the solvatochromic behavior was also an important aspect to investigate the polarity of chromophores. It was found that both chromophores B and C showed a very large

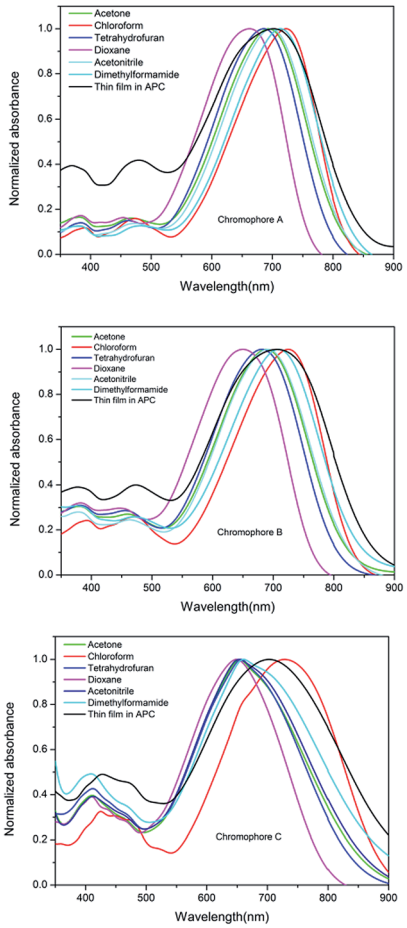

Fig. 2 UV-Vis absorption spectra of chromophores A, B and C in six kinds of aprotic solvents with varying dielectric constants (ε).

bathochromic shift of 79 nm, from dioxane to chloroform, displaying larger solvatochromism than that of CLD (60 nm) and a similar single donor FTC (61 nm) chromophore,[21,22] while chromophore A showed a moderate bathochromic shift of 61 nm from dioxane to chloroform. This confirms that chromophores B and C are more easily polarizable than A although chromophore A had a similar pyrrole bridge to chromophore B.[23] It is interesting to note that on continuous increase of the dielectric constant of the solvent beyond that of chloroform, the NLO chromophore exhibited negative solvatochromism. For example, compounds A and B showed hypsochromic shifts of −31 nm and −36 nm, respectively, from chloroform to acetone. Chromophore C also exhibited similar solvatochromic behavior. Such a phenomenon was reported by Davies[23] and was ascribed to the back electron transfer from the acceptor side to the donor side in polar solvents which caused a blue-shift from the absorption. The same explanation should also hold for the present series of NLO chromophores.[24]

The photoluminescence emission spectra of A, B and C were also measured in different organic solvents. The spectral data are summarized in Table 1. Chromophores A, B and C showed Stokes shifts of 137 nm, 157 nm, and 228 nm in dioxane, and 130 nm, 139 nm, 223 nm in chloroform respectively. Chromophore C

Table 1 Optical property data of the chromophores

	Ultraviolet spectrum				Fluorescence spectrum		
Chromophores	λ_{max}[a] (nm)	λ_{max}[b] (nm)	$\Delta\lambda$[c] (nm)	λ_{max}[d] (nm)	λ_{max}[e] (nm)	λ_{max}[f] (nm)	$\Delta\lambda$[g] (nm)
A	662	723	61	702	799	853	54
B	646	725	79	706	803	864	61
C	649	728	79	703	877	951	74

[a] λ_{max} was measured in dioxane. [b] λ_{max} was measured in chloroform. [c] $\Delta\lambda$ was the difference between [a] λ_{max} and [b] λ_{max}. [d] λ_{max} was measured in films. [e] λ_{max} was measured in dioxane. [f] λ_{max} was measured in chloroform. [g] $\Delta\lambda$ was the difference between [e] λ_{max} and [f] λ_{max}.

showed larger Stokes shifts than that of chromophores A and B. Chromophore A showed the smallest Stokes shifts.

2.4 Theoretical calculations and redox properties

The DFT calculations were carried out at the hybrid B3LYP level by employing the split valence 6-311g (d, p) basis set[25,26] to understand the ground-state polarization of the chromophores with different bridges. When used carefully and consistently, this method of DFT has been shown to give relatively consistent descriptions of first-order hyperpolarizability for a number of similar chromophores.[7,26] In order to compare the microscopic nonlinear effect between chromophores, the β value of chromophore D was also calculated. All molecules were assumed to be in *trans*-configurations. The HOMO–LUMO energy gaps, dipole moment (μ), and first hyperpolarizability (β) of the chromophores obtained from DFT calculations are summarized in Table 2.

For chromophores A and B, the additional electron acceptors (–Br, $-NO_2$) created another local dipole moment which results in a larger total dipole moment than that of chromophore D. As reported previously, the β value has a close relationship with the strength of the donor and acceptor end groups and with the nature and length of the bridge, substituents, steric hindrance and intramolecular charge-transfer and so on.[27,28] Chromophore C showed the largest β value of all the four chromophores. This might be due to the molecular configuration and different combination effects among the donor, acceptor and bridge. The location of the heterocyclic ring also plays a critical role in determining β values, other than the nature of the ring.[29] Pyrrole, being the most electron rich five-membered heteroaromatic ring, may counteract the electron-withdrawing effect of the acceptor perhaps resulting in a decreased β value of chromophores A, B and D.[30]

Optimization of the molecular first hyperpolarizability of dipolar EO chromophores relies on tuning of the electron density distribution through chemical modification of molecular constituents.[31] It may be noted that, though having a similar pyrrole bridge, the β values of chromophores A and B were nearly 20% higher than that of chromophore D. This can be explained by that the abundant electron density of the pyrrole ring would be weakened by modified benzene ring groups which may lead to increased β values. The additional electron acceptor incorporated into the conjugated system may facilitate the electron transfer from the donor to the acceptor, thus decreasing the energy barrier of the charge transfer transition which leads to an increased β value. From another perspective, the enhanced β values of chromophores A and B might be also ascribed to the fact that the additional electron acceptor group added perpendicular to the conjugated backbone could serve as an efficient spacer to reduce the formation of dipole couples.[15,32] This may prove that the special "auxiliary acceptor" group introduced perpendicular to the conjugated backbone could increase the β values.

In order to determine the redox properties of chromophores A–C, cyclic voltammetry (CV) measurements were conducted in degassed anhydrous acetonitrile solutions containing 0.1 mol L^{-1} tetrabutylammonium hexafluorophosphate (TBAPF) as the supporting electrolyte. The relative data of 1×10^{-4} mol L^{-1} chromophores A–C were recorded, as shown in Table 2. The HOMO and LUMO levels of all three chromophores can be calculated from their corresponding oxidation and reduction potentials.[33] The difference between these two values provides the HOMO–LUMO energy difference ΔE (CV). The calculation

Table 2 Summary of DFT and electro-chemical data

Chromophore	ΔE (DFT)[a] (eV)	ΔE (CV)[b] (eV)	E_{ox}[c] (V)	E_{red}[d] (V)	μ[e]/D	β_{tot}[f] (10^{-30} esu)
A	2.02	1.36	0.12	−1.24	20.51	672.35
B	1.90	1.34	0.11	−1.23	21.62	686.10
C	1.96	1.35	0.09	−1.26	20.84	809.49
D	2.04	—	—	—	18.54	571.83

[a] ΔE (DFT) was calculated from DFT calculations. [b] ΔE (CV) was calculated from their corresponding oxidation and reduction potentials. [c] Referenced to the ferrocene standard. [d] Referenced to the ferrocene standard. [e] μ is the total dipole moment. [f] β_{tot} is the first-order hyperpolarizability, where $\beta_{tot} = \sqrt{(\beta_x)^2 + (\beta_y)^2 + (\beta_z)^2}$ is calculated from DFT quantum mechanical methods.

results are summarized in Table 2. The HOMO levels of chromophores A–C were estimated to be −4.92, −4.91, and −4.89 eV, which showed a slight increase. In the meantime, the corresponding LUMO level of A–C only showed slight changes of about −3.56, −3.57, and −3.54 eV, respectively. The HOMO–LUMO gap was the lowest for chromophore B (1.34 eV) and the highest for chromophore A (1.36 eV). The narrower energy gap indicated easier charge transfer.[34,35]

The HOMO–LUMO energy gaps ΔE (DFT) were also calculated by DFT calculations as shown in Table 2. The energy gaps between the HOMO and LUMO energy for chromophores A, B, and C were 2.02, 1.90, and 1.96 eV. The electrochemical values are corroborated by the DFT calculations. Trends of energy gaps between ΔE (DFT) and ΔE (CV) for the chromophores were found to be consistent. As is commonly observed, ΔE (DFT) is significantly overestimated when compared to the data obtained by CV.

The frontier molecular orbitals are often used to obtain information about the optical and electrical properties of molecules.[34] Fig. 3 depicts the electron density distribution of the HOMO and LUMO structures which indicated that the density of the ground and excited state electron is asymmetric along the dipolar axis of the chromophores.

To get more information from the frontier orbitals, the composition of the HOMOs and LUMOs has been calculated using the Multiwfn program.[36] The whole chromophore molecule was segmented as a donor, a π-bridge, and an acceptor as shown in Table 3. For the chromophores A–D, the LUMO was largely stabilized by the contributions from the acceptor (43.70–47.08%) and the π-bridge (36.64–39.51%), while the HOMO was largely stabilized by the contributions from donors (56.82–59.42%) and the π-bridge (24.57–25.44%). The contribution of acceptors of chromophores A, B and D (46.81–47.08%) containing a pyrrole-based bridge seemed to be bigger than that of chromophore C (43.70%) with a thiophene-bridge for the LUMO level. As for the HOMO level, the acceptors of chromophores A, B and D also contributed more than that of chromophore C.

2.5 Electro-optic performance

The computational approach has helped to assess the relationship between bulk and molecular level non-linear optical (NLO) effects. For dipolar chromophores in an electric poling field, the electro-optic coefficient in the direction of the applied field is related to the molecular first hyperpolarizability by[37]

$$r_{33} = |2Nf(\omega)\beta\langle\cos^3\theta\rangle/n^4|$$

where N is the chromophore number density (molecules per cm^3) in the polymer host, n is the index of refraction of the chromophore-containing polymeric material, and $f(\omega)$ is the product of local-field (Debye–Onsager) factors. $\cos^3(\theta)$ is the acentric order parameter. θ is the angle between the permanent dipole moment of chromophores and the applied electric field. At low concentration, the electro-optic activity increased with chromophore density, dipole moment and the strength of the electric poling field. However, when the concentrations of chromophores increased to a certain extent, the N and $\cos^3(\theta)$ are no longer independent factors. Then,

$$\langle\cos^3(\theta)\rangle = (\mu F/5kT)[1 - L^2(W/kT)]$$

where k is the Boltzmann constant and T is the Kelvin (poling) temperature. $F = [f(0)E_P]$ where E_p is the electric poling field. L is the Langevin function, which is a function of W/kT, the ratio of the intermolecular electrostatic energy (W) to the thermal energy (kT). L is related to electrostatic interactions between molecules.

This relationship can be successfully applied to qualitatively predict the important trends involving electro-optic activity although not the quantitative values of electro-optic coefficients. When the intermolecular electrostatic interactions are neglected, the electro-optic coefficient (r_{33}) should increase linearly with chromophore density, dipole moment, first hyperpolarizability and the strength of the electric poling field. But chromophores with large dipole moments generate an intermolecular static electric field dipole–dipole interaction, which leads to the unfavorable antiparallel packing of chromophores. So the number of truly oriented chromophores (N) is small. In molecular optimization, introducing a huge steric hindrance group to isolate chromophores is the most popular and easy way to attenuate the dipole–dipole interactions of chromophores.[38]

To achieve a high EO coefficient, the chromophore should have facile intra-charge transfer ability. The π–π stacking interactions and inter-molecular charge transport between

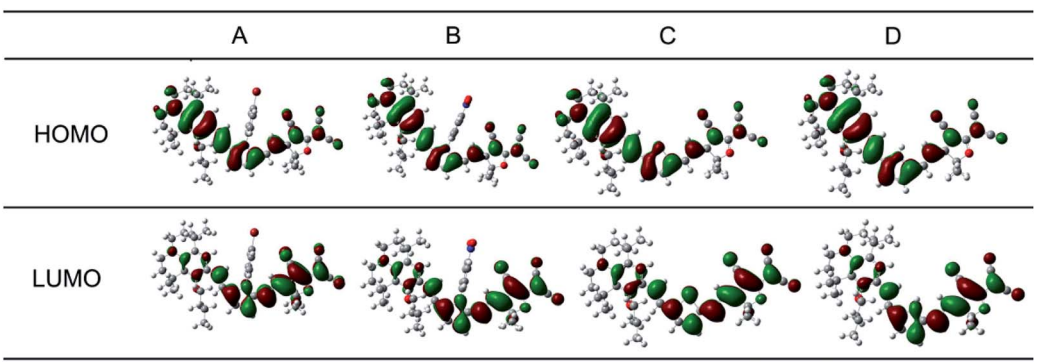

Fig. 3 The frontier molecular orbitals of chromophores A–D.

Table 3 The molecular orbital composition (%) in the ground state for chromophores A–D[a]

	A		B		C		D	
Chromophore	HOMO	LUMO	HOMO	LUMO	HOMO	LUMO	HOMO	LUMO
Donor	56.82%	16.28%	57.82%	16.39%	59.42%	16.79%	56.77%	16.22%
π bridge	25.02%	36.64%	24.57%	36.80%	25.44%	39.51%	24.75%	36.95%
Acceptor	18.16%	47.08%	17.61%	46.81%	15.14%	43.70%	18.48%	46.83%

[a] The molecular orbital composition was calculated using the Multiwfn program with Ros-Schuit (SCPA) partition.

chromophores should be reduced in order to translate the microscopic hyperpolarizability into a macroscopic EO response more effectively. In order to balance the steric hindrance and the molecular free mobility for chromophore acentric alignment in the guest–host EO polymer, the poling conditions should be carefully explored.[38]

In order to investigate the translation of the microscopic hyperpolarizability into a macroscopic EO response, the polymer films doped with different concentrations of chromophores into amorphous polycarbonate (APC) were prepared using dibromomethane as solvent. The resulting solutions were filtered through a 0.2 μm PTFE filter and spin-coated onto indium tin oxide (ITO) glass substrates. Films of doped polymers were baked at 80 °C in a vacuum oven overnight. The corona poling process was carried out at a temperature of 10 °C above the glass transition temperature (T_g) of the polymer. The r_{33} values of poled films were measured by the Teng–Man simple reflection method at a wavelength of 1310 nm using a carefully selected thin ITO electrode with low reflectivity and good transparency in order to minimize the contribution from multiple reflections.[39,40]

To evaluate their EO activities, 10 wt% of the chromophores A–C were doped into APC and formulated as the typical guest–host polymer. For this series of chromophores, the poled films of A/APC, B/APC and C/APC afforded r_{33} values of 40, 53 and 60 pm V^{-1}, respectively. To identify the underlying mechanism for the difference in achievable EO performance, the order parameter (Φ) was calculated by measuring UV-Vis absorption spectra. After the corona poling, the dipole moments of the chromophore moieties in the polymer were aligned, and the absorption curve decreased due to birefringence.[17] The order parameter (Φ) for films can be calculated from the absorption

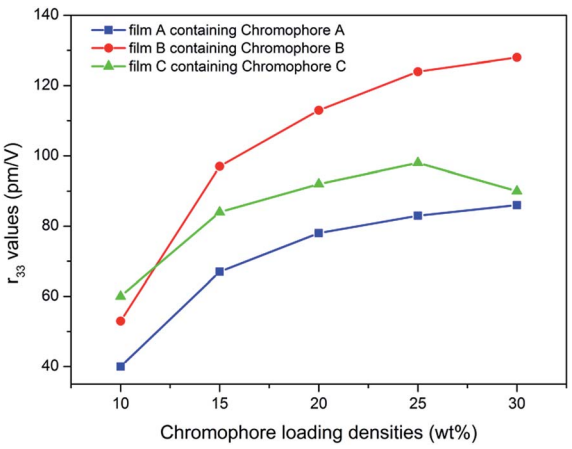

Fig. 4 r_{33} values of NLO thin films as a function of chromophore loading densities.

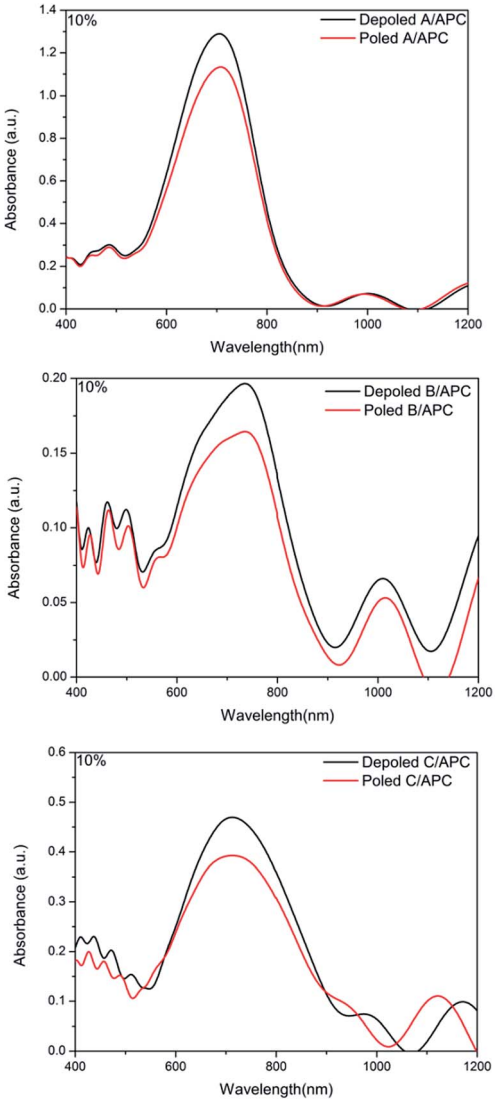

Fig. 5 UV-Vis absorption spectra of EO polymers before and after poling (10 wt%).

changes according to the following equation: $\Phi = 1 - A/A_0$,[41] in which A and A_0 are the respective absorptions of the polymer films after and before corona poling. The order parameter (Φ) of poled films was calculated. The Φ values of films A/APC, B/APC, and C/APC are 12.12%, 16.28%, 16.34%, respectively as shown in Fig. 5. The larger order parameters of films B and C indicate that films B/APC and C/APC were more easily poled than film-A/APC. The film-C/APC achieved the largest r_{33} value probably due to its largest β and good polarizability. With relatively low β, the r_{33} value of film-B/APC was smaller than that of film-C/APC. The drop in EO activity from film-B/APC to film-A/APC is mainly associated with the lowest β of chromophore A in the polar polymer matrix and the inefficient poling, because of its lower polarizability than the other two chromophores. This corresponded well with the results of the solvatochromism study, DFT calculations and redox properties of chromophores.

The r_{33} values of films A/APC, B/APC, and C/APC were measured at different loading densities, as shown in Fig. 4. As a result, the r_{33} values of film-C/APC were gradually improved from 60 pm V^{-1} (10 wt%) to 98 pm V^{-1} (25 wt%), while the r_{33} values dropped to 90 pm V^{-1} as the loading density increased from 25 wt% to 30 wt%. The r_{33} values of film-B/APC were improved from 53 pm V^{-1} (10 wt%) to 128 pm V^{-1} (30 wt%). A similar trend was also observed for film-A/APC whose r_{33} values increased from 40 pm V^{-1} (10 wt%) to 86 pm V^{-1} (30 wt%). When the concentration of the chromophore in APC is low, film C/APC displayed a larger r_{33} value than that of the film B/APC. As the chromophore loading increased, this trend is reversed. This can be explained by that, when in a low-density range, the intermolecular dipolar interactions are relatively weak. The intermolecular dipole–dipole interactions would become stronger and stronger, accompanied by the increased concentration of NLO chromophore moieties in the polymer which would finally lead to a decreased NLO coefficient. The introduction of side-groups attached to the conjugated π-system can make inter-chromophore electrostatic interactions less favorable.[10,42]

The Φ values of films A/APC, B/APC, and C/APC which contain 25 wt% of the chromophores are 18.02%, 20.38%, 17.26%, respectively, while the Φ values of films A/APC, B/APC, and C/APC are 18.67%, 21.03%, 15.85%, respectively, with a high loading of 30 wt% (see ESI†). The difference in the order parameter indicates that films A/APC and B/APC have weaker inter-chromophore electrostatic interactions than film-C/APC in high density. It may be revealed by the optimized configurations (Fig. 6) that the side benzene ring groups were perpendicular to the direction of the dipole moment of the chromophore which could act as the isolation group to suppress the possible aggregation. The film B/APC achieves the largest r_{33} value of 128 pm V^{-1}, even though it has lower β. The high saturated loading density and larger Φ values of films A and B were probably attributed to the fact that the chromophore structure isolated the chromophores from each other more effectively, thus improving the NLO effect at a higher chromophore loading density level.

Based on the above points, chromophores A and B containing a modified pyrrole bridge can translate their large β values into bulk EO activities more effectively than chromophore C due to the isolation of modified benzene ring groups. However, the different r_{33} values of film-A/APC and film B/APC prove that the different auxiliary acceptor groups (–Br, $–NO_2$) showed different influences on molecular properties. Moreover, the large r_{33} values of the chromophores show that the modified pyrrole bridges were stable enough to withstand high temperatures encountered in electric field poling and subsequent processing of chromophore/polymer materials.

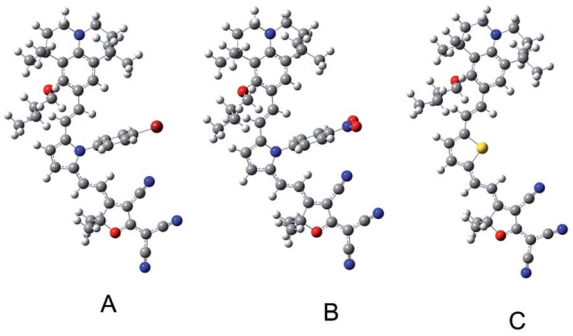

Fig. 6 The optimized structure of chromophores A, B and C.

3. Conclusion

Three organic NLO chromophores with pyrrole or thiophene bridges have been synthesized and systematically characterized. The new chromophores showed high thermal and chemical stabilities, large nonlinear optical coefficient, and good solubility in all common solvents. The pyrrole moiety bridge has been substituted with modified phenyl groups. The introduction of the side phenyl groups helps to improve the chemical and thermal stability of the unstable pyrrole moiety, so that it could be used in electro-optic (OEO) materials. Moreover the side groups can reduce dipole–dipole interactions so as to translate their hyperpolarizability (β) values into bulk EO performance more effectively than chromophore C. DFT calculations suggested that the modified electron acceptor groups (–Br, $–NO_2$) in chromophores A and B could increase the β value, and they showed different influences on the solvatochromic behavior, thermal stability, and electro-optic activity of the chromophores. Incorporation of chromophores A and B into APC provided large electro-optic coefficients of 86 and 128 pm V^{-1} at 1310 nm with a high loading of 30 wt%. All these might be useful in designing other new NLO chromophores with a modified pyrrole bridge to optimize the molecular structure for achieving different properties. These novel modified pyrrole bridges will show promising applications in nonlinear optical (NLO) chromophore synthesis.

4. Experimental section

4.1 Materials and instrument

All chemicals are commercially available and are used without further purification unless otherwise stated. *N*,*N*-Dimethyl formamide (DMF), phosphorusoxychloride ($POCl_3$), tetrahydrofuran (THF) and ether were distilled over calcium hydride

and stored over molecular sieves (pore size 3 Å). 1-(4-Bromophenyl)-1*H*-pyrrole-2-carbaldehyde (**1a**) was prepared according to the literature.[43] 1-(4-Nitrophenyl)-1*H*-pyrrole-2-carbaldehyde (**1b**) was prepared according to the literature.[44] The 2-dicyanomethylene-3-cyano-4-methyl-2,5-dihydrofuran (TCF) acceptor was prepared according to the literature.[45] Compounds **2a** and **2b** were prepared according to the literature.[46] TLC analyses were carried out on 0.25 mm thick precoated silica plates and spots were visualized under UV light. Chromatography on silica gel was carried out on Kieselgel (200–300 mesh).

4.2 Measurements and instrumentation

^{1}HNMR spectra were recorded using an Advance Bruker 400 M (400 MHz) NMR spectrometer (tetramethylsilane as internal reference). The MS spectra were obtained using MALDI-TOF (Matrix Assisted Laser Desorption/Ionization of Flight) on a BIFLEXIII (Broker Inc.) spectrometer. The UV-Vis spectra were recorded on a Cary 5000 photospectrometer. The TGA was determined using a TA5000-2950TGA (TA co) with a heating rate of 10 °C min^{-1} under the protection of nitrogen. Cyclic voltammetric data were measured on a BAS CV-50W voltammetric analyzer using a conventional three-electrode cell with Pt metal as the working electrode, a Pt gauze as the counter-electrode, and Ag/$AgNO_3$ as the reference electrode at a scan rate of 50 mV s^{-1}. 0.1 M Tetrabutylammonium hexa-fluorophosphate (TBAPF) in acetonitrile is the electrolyte. The fluorescence spectra were recorded on a Hitachi F-4500 fluorescence spectrometer. The elemental analysis was performed on a Flash EA 1112 elemental analyzer. The melting points were obtained using a TA DSC Q10 under N_2 at a heating rate of 10 °C min^{-1}.

4.3 Synthesis and characterization

Compound 4. Under a N_2 atmosphere, anhydrous potassium carbonate (6.4 g, 40 mmol) was added to a solution of compound **3** (5.46 g, 20 mmol) and compound C_4H_9Br (4.11 g, 30 mmol) in DMF (120 mL). The mixture was allowed to stir at 120 °C for 12 h and then poured into water. The organic phase was extracted using AcOEt, washed with brine and dried over $MgSO_4$. After removal of the solvent under reduced pressure, the crude product was purified by silica chromatography, eluting with acetone : hexane = 1 : 10 to give compound **4** as a yellow powder with 91.3% yield (6.02 g, 18.26 mmol). ^{1}H NMR (400 MHz, acetone) δ 9.90 (1H, s, CHO), 7.48 (1H, s, ArH), 3.96 (2H, t, J = 6.8 Hz, OCH_2), 3.36–3.33 (2H, m, NCH_2), 3.30–3.26 (2H, m, NCH_2), 1.86 (2H, dd, J = 14.9, 7.0 Hz, CH_2), 1.76–1.66 (4H, m, CH_2), 1.52 (2H, dt, J = 14.8, 7.5 Hz, CH_2), 1.41 (6H, s, CH_3), 1.23 (6H, s, CH_3), 0.99 (3H, t, J = 7.4 Hz, CH_3); MS (EI) (M^+, $C_{21}H_{31}NO_2$): calcd: 329.4837; found: 329.2485. m.p.: 223.83 °C.

Compound 5a. Under a N_2 atmosphere, to a solution of compound **4** (0.99 g, 3 mmol) and **3a** (2.08 g, 3.6 mmol) in ether (100 mL) was added NaH (0.43 g, 18 mmol). The solution was allowed to stir for 48 h and then poured into water. The organic phase was extracted using AcOEt, washed with brine and dried over $MgSO_4$. After removal of the solvent under reduced pressure, the crude product was purified by silica chromatography, and eluted with acetone : hexane = 1 : 20 to give compound **5a** as an orange oil in 83.7% yield (1.37 g, 2.51 mmol). ^{1}H NMR (400 MHz, acetone) δ 7.60 (2H, d, J = 6.6Hz, ArH), 7.38 (1H, d, J = 8.7 Hz, CH), 7.23 (2H, d, J = 6.6 Hz, ArH), 7.08 (1H, s, ArH), 6.87 (1H, d, J = 8.7, CH), 6.32 (1H, d, J = 11.9 Hz, PrH), 6.23–6.18 (1H, m, PrH), 6.11 (1H, d, J = 11.9 Hz, PrH), 3.61 (2H, t, J = 6.7 Hz, OCH_2), 3.13–3.09 (2H, m, NCH_2), 3.08–3.02 (1H, m, NCH_2), 1.70 (6H, m, CH_2), 1.52–1.42 (2H, m, CH_2), 1.36 (6H, s, CH_3), 1.10 (6H, s, CH_3), 0.95 (3H, t, J = 7.3 Hz, CH_3); MS (MALDI) (M^+, $C_{32}H_{39}BrN_2O$): calcd: 547.573; found: 547.258.

Compound 5b. The procedure for compound **5a** was followed to prepare **5b** from **4** and **3b** as a red oil in 56.7% yield (0.87 g, 1.71 mmol). ^{1}H NMR (400 MHz, acetone) δ 8.40 (2H, d, J = 9.9 Hz, ArH), 7.71 (2H, d, J = 9.9 Hz, ArH), 7.17 (1H, s, PrH), 7.08 (1H, s, ArH), 7.01 (1H, d, J = 16.2 Hz, CH), 6.69 (1H, d, J = 16.2 Hz, CH=), 6.58 (1H, d, J = 3.4 Hz, PrH), 6.34 (1H, t, J = 3.4 Hz, PrH), 3.83 (2H, t, J = 6.6 Hz, OCH_2), 3.16–3.11 (2H, m, NCH_2), 3.10–3.05 (2H, m, NCH_2), 1.77 (2H, dd, J = 14.5, 7.4 Hz, CH_2), 1.73–1.65 (4H, m, CH_2), 1.51 (2H, dd, J = 15.1, 7.4 Hz, CH_2), 1.39 (6H, s, CH_3), 1.18 (6H, s, CH_3), 0.96 (3H, t, J = 7.4 Hz, CH_3); MS (MALDI): m/z (M^+, $C_{32}H_{39}N_3O_3$): calcd: 513.073; found: 513.098.

Compound 5c. The procedure for compound **5a** was followed to prepare **5c** from **4** and **3c** as an orange oil in 86.3% yield (1.06 g, 2.59 mmol). The ratio of the Z : E isomer is 50 : 50% calculated by the integration of respective protons. ^{1}H NMR (400 MHz, $CDCl_3$) δ 7.16 (1H, m, PrH), 7.09 (1H, d, J = 5.0 Hz, PrH), 7.07 (1H, d, J = 5.0 Hz, PrH), 7.04 (0.5H, d, J = 3.4 Hz, CH), 6.98 (1H, s, ArH), 6.91 (1H, d, J = 3.6 Hz, CH), 6.57 (0.5H, d, J = 11.8 Hz, CH), 6.48 (0.5H, d, J = 11.8 Hz, CH_2), 3.89 (2H, m, OCH_2), 3.19–3.13 (2H, m, NCH_2), 3.13–3.05 (2H, m, NCH_2), 1.93–1.80 (2H, m, CH_2), 1.80–1.71 (4H, m, CH_2), 1.58 (3H, m, CH_2), 1.44 (3H, s, CH_3), 1.43 (3H, s, CH_3), 1.31 (3H, s, CH_3), 1.17 (3H, s, CH_3), 1.01 (1.5H, t, J = 7.4 Hz, CH_3), 0.94 (1.5H, t, J = 7.4 Hz, CH_3); MS (MALDI) (M^+, $C_{26}H_{35}NOS$): calcd: 410.045; found: 410.033.

Compound 6a. DMF (0.42 g, 5.75 mmol) was added to freshly distilled $POCl_3$ (0.59 g, 3.84 mmol) under an atmosphere of N_2 at 0 °C, and the resulting solution was stirred until its complete conversion into a glassy solid. After the addition of **5a** (1.40 g, 2.56 mmol) in 1,2-dichloroethane (60 mL) dropwise, the mixture was stirred at room temperature overnight, then poured into a saturation aqueous solution of sodium acetate (300 mL). After 2 hour stirring at room temperature, the mixture extracted with chloroform (5 × 30 mL), and the organic fractions were collected and dried over anhydrous $MgSO_4$. The crude product was purified through silica gel chromatography and eluted with acetone : hexane = 1 : 5 to afford a red solid **6a** in 73.2% yield (1.08 g, 1.87 mmol). ^{1}H NMR (400 MHz, acetone) δ 9.38 (1H, s, CHO), 7.71 (2H, d, J = 8.4 Hz, ArH), 7.33 (2H, d, J = 8.4 Hz, ArH), 7.26 (1H, d, J = 16.3 Hz, CH), 7.14 (1H, d, J = 4.2 Hz, PrH), 7.05 (1H, s, ArH), 6.73 (1H, d, J = 4.2 Hz, PrH), 6.39 (1H, d, J = 16.3 Hz, CH), 3.78 (2H, t, J = 6.7 Hz, OCH_2), 3.19–3.14 (2H, m, NCH_2), 3.13–3.07 (2H, m, NCH_2), 1.76 (2H, dd, J = 14.3, 7.2 Hz, CH_2), 1.72–1.64 (4H, m, CH_2), 1.52 (2H, dd, J = 14.3, 7.2 Hz, CH_2), 1.38 (6H, s, CH_3), 1.15 (6H, s, CH_3), 0.99 (3H, t, J = 7.3 Hz, CH_3); ^{13}C NMR (101 MHz, acetone) δ 176.77, 156.37, 143.58, 142.74, 136.97, 133.39, 132.16, 130.55, 129.92, 126.37, 123.36, 122.04,

117.58, 110.78, 106.66, 74.45, 47.09, 46.29, 40.37, 36.64, 32.60, 32.18, 32.02, 30.70, 29.95, 19.43, 13.77; MS (MALDI) (M^+, $C_{33}H_{39}BrN_2O_2$): calcd: 575.867; found: 575.957.

Compound 6b. The procedure for compound **6a** was followed to prepare **6b** from **5b** as a red solid in 71.8% yield (0.99 g, 1.84 mmol). ^{1}H NMR (400 MHz, acetone) δ 9.44 (1H, s, CHO), 8.43 (2H, d, J = 8.9 Hz, ArH), 7.69 (2H, d, J = 8.9 Hz, ArH), 7.32 (1H, d, J = 16.2 Hz, CH), 7.24 (1H, d, J = 4.2 Hz, PyH), 7.07 (1H, s, ArH), 6.81 (1H, d, J = 4.2 Hz, PyH), 6.41 (1H, d, J = 16.2 Hz, CH), 3.79 (2H, t, J = 6.7 Hz, NCH_2), 3.79 (2H, t, OCH_2), 3.18(2H, t, NCH_2),3.13(2H, t, NCH_2), 1.79–1.73 (2H, m, CH_2), 1.72–1.63 (4H, m, CH_2), 1.52 (2H, m, 7.6 Hz, CH_2), 1.38 (6H, s, CH_3), 1.14 (6H, s, CH_3), 0.99 (3H, t, CH_3); ^{13}C NMR (101 MHz, $CDCl_3$) δ 176.77, 156.33, 147.21, 143.66, 143.09, 132.30, 131.18, 129.17, 124.01, 122.53, 109.34, 107.36, 74.77, 47.20, 46.68, 39.87, 36.10, 32.51, 32.07, 31.95, 30.77, 29.93, 19.28, 13.90; MS (MALDI) (M^+, $C_{33}H_{39}N_3O_4$): calcd: 541.136; found: 541.138.

Compound 6c. Under a N_2 atmosphere, **5c** (0.41 g, 1 mmol) was dissolved in 150 mL of freshly distilled THF and cooled to −78 °C. Approximately 2 equivalents of BuLi in hexane (20 mL, 5 mmol) was added dropwise over 20 min. Reaction continued at −78 °C for 1 h at which time DMF (0.37 g, 5 mol) was added over 1 min. The reaction was allowed to reach RT while the solution was stirred for 1 h. The organic phase was extracted by AcOEt, washed with brine and dried over $MgSO_4$. After removal of the solvent under reduced pressure, the crude product was purified by silica chromatography and eluted with acetone : hexane = 1 : 5 to give compound **6c** as an orange oil in 75.6% yield (0.33 g, 0.76 mmol). ^{1}H NMR (400 MHz, $CDCl_3$) δ 9.82 (1H, s, CHO), 7.64 (1H, d, J = 3.9 Hz, CH), 7.33 (1H, d, J = 16.1 Hz, CH), 7.27 (1H, d, J = 5.9 Hz, CH), 7.05 (1H, d, J = 5.9 Hz, CH), 6.96 (1H, d, J = 16.1 Hz, CH), 3.84 (2H, t, J = 6.7 Hz, OCH_2), 3.23–3.19 (2H, m, NCH_2), 3.16–3.12 (2H, m, CH_2), 1.91–1.83 (2H, m, CH_2), 1.77–1.72 (4H, m, CH_2), 1.60–1.53 (2H, m, CH_2), 1.43 (6H, s, CH_3), 1.31 (6H, s, CH_3), 1.01 (3H, t, J = 7.3 Hz, CH_3); ^{13}C NMR (101 MHz, $CDCl_3$) δ 181.23, 155.85, 153.99, 138.83, 136.30, 121.99, 123.33, 121.32, 114.32, 66.95, 46.41, 45.74, 39.11, 35.43, 31.70, 31.27, 30.14, 29.88, 29.02 28.68, 24.50, 21.53, 18.54, 13.10; MS (MALDI) (M^+, $C_{27}H_{35}NO_2S$): calcd: 437.347; found: 437.181.

Chromophore A. To a solution of **6a** (0.29 g, 0.50 mmol) and the TCF acceptor (0.12 g, 0.60 mmol) in MeOH (60 mL) were added several drops of triethylamine. The reaction was allowed to stir at 78 °C for 5 h. The reaction mixture was cooled and green crystal precipitation was facilitated. After removal of the solvent under reduced pressure, the crude product was purified by silica chromatography and eluted with AcOEt : hexane = 1 : 5 to give chromophore A as a green solid in 32.3% yield (0.12 g, 0.16 mmol). ^{1}H NMR (400 MHz, acetone) δ 8.11 (1H, d, J = 15.6 Hz, CH), 7.62 (2H, d, J = 9.5 Hz, ArH), 7.36 (2H, d, J = 9.5 Hz, ArH), 7.22 (1H, s, ArH), 7.05 (1H, d, J = 3.3 Hz, PyH), 6.90 (1H, d, J = 3.3 Hz, PyH), 6.83 (1H, d, J = 15.6 Hz, CH), 6.76 (2H, s, CH), 3.62 (2H, t, J = 6.6 Hz, OCH_2), 3.15–3.09 (2H, m, NCH_2), 3.08–3.02 (2H, m, NCH_2), 1.67 (6H, s, CH_3), 1.58 (6H, m, CH_2), 1.53–1.44 (2H, m, CH_2), 1.26 (6H, s, CH_3), 1.10 (6H, s, CH_3), 0.76 (3H, t, J = 8.5 Hz, CH_3); ^{13}C NMR (101 MHz, acetone) δ 175.06, 156.38, 143.69, 141.90, 140.50, 137.93, 133.55, 132.25, 126.65, 126.65, 122.63, 121.75, 121.39, 120.81, 116.84, 112.30, 111.55, 111.26, 109.93, 109.08, 107.86, 97.03, 92.50, 74.17, 53.50, 52.28, 46.44, 45.91, 39.63, 35.84, 31.96, 31.47, 29.91, 25.05, 18.57, 12.98; MS (MALDI) (M^+, $C_{44}H_{46}BrN_5O_2$): calcd: 756.776; found: 756.686. m.p.: 189.48 °C. Anal. calcd (%) for $C_{44}H_{46}BrN_5O_2$: C, 69.83; H, 6.13; N, 9.25; found: C, 70.03; H, 6.17; N, 9.22.

Chromophore B. The procedure for chromophore A was followed to prepare chromophore B from **6b** as a green solid in 33.9% yield (0.12 g, 0.17 mmol). The ratio of the Z : E isomer was 50 : 50% calculated by the integration of respective protons. ^{1}H NMR (400 MHz, acetone) δ 8.57 (1H, d, J = 8.9 Hz, ArH), 8.44 (1H, d, J = 6.9 Hz, ArH), 8.22 (0.5H, d, J = 15.7 Hz, CH), 7.85 (2H, d, J = 8.9 Hz, ArH), 7.69 (0.5H, d, J = 4.6 Hz, CH), 7.60 (0.5H, d, J = 15.4 Hz, CH), 7.47 (0.5H, d, J = 16.1 Hz, CH), 7.38 (0.5H, s, PrH), 7.33 (0.5H, d, J = 3.4 Hz, CH), 7.14 (0.5H, s, PrH), 7.12 (0.5H, d, J = 4.7 Hz, CH), 7.11 (0.5H, d, J = 3.4 Hz, CH), 7.01 (0.5H, d, J = 15.7 Hz, CH), 6.95 (1H, s, ArH), 6.63 (0.5H, d, J = 15.4 Hz, CH), 6.55 (0.5H, d, J = 16.1 Hz, CH), 3.78 (2H, dd, J = 11.9, 6.6 Hz, OCH_2), 3.27–3.22 (2H, m, NCH_2), 3.18 (2H, dd, J = 5.9, 4.5 Hz, NCH_2), 1.81 (3H, s, CH_3), 1.77–1.64 (6H, m, CH_2), 1.64 (3H, s, CH_3), 1.51 (2H, m, CH_2), 1.38 (6H, s, CH_3), 1.22 (3H, s, CH_3), 1.14 (3H, s, CH_3), 0.98 (1.5H, t, J = 7.4 Hz, CH_3), 0.87 (1.5H, t, J = 7.4 Hz, CH_3); ^{13}C NMR (101 MHz, acetone) δ 176.35, 156.68, 146.30, 143.99, 141.73, 140.94, 134.07, 133.36, 132.59, 132.16, 129.84, 125.91, 124.83, 124.54, 123.18, 122.70, 121.77, 121.59, 121.57, 116.46, 111.42, 109.07, 106.94, 97.24, 96.35, 74.31, 64.49, 46.46, 45.90, 39.43, 35.69, 31.94, 31.54, 31.35, 29.87, 29.61, 24.85, 18.73, 13.00; MS (MALDI) (M^+, $C_{44}H_{46}N_6O_4$): calcd: 722.878 found: 722.902. m.p.: 195.98 °C. Anal. calcd (%) for $C_{44}H_{46}N_6O_4$: C, 73.11; H, 6.41; N, 11.63; found: C, 73.20; H, 6.43; N, 11.67.

Chromophore C. The procedure for chromophore A was followed to prepare chromophore C from **6c** as a green solid in 68.9% yield (0.21 g, 0.34 mmol). ^{1}H NMR (400 MHz, $CDCl_3$) δ 7.73 (1H, d, J = 15.5 Hz, CH), 7.31 (1H, d, J = 4.0 Hz, CH), 7.26 (1H, d, J = 15.9 Hz, CH), 7.19 (1H, s, ArH), 6.96 (1H, d, J = 4.0 Hz, CH), 6.92 (1H, d, J = 15.9 Hz, CH), 6.44 (1H, d, J = 15.5 Hz, CH), 3.78 (2H, t, J = 6.7 Hz, OCH_2), 3.22–3.15 (2H, m, NCH_2), 3.14–3.07 (2H, m, NCH_2), 1.67 (6H, s, CH_3), 1.57–1.46 (8H, m, CH_2), 1.24 (6H, s, CH_3), 1.19 (6H, s, CH_3), 0.96 (3H, t, J = 7.4 Hz, CH_3); ^{13}C NMR (101 MHz, $CDCl_3$) δ 174.88, 171.68, 154.84, 154.83, 154.68, 138.30, 136.77, 136.10, 130.76, 126.29, 126.27, 125.61, 122.13, 114.58, 110.25, 110.16, 110.11, 95.80, 94.39, 74.74, 54.46, 46.61, 46.09, 38.73, 35.00, 31.72, 31.26, 29.90, 28.34, 25.53, 18.59, 13.09; MS (MALDI) (M^+, $C_{38}H_{42}N_4O_2S$): calcd: 618.186; found: 618.204. m.p.: 197.56 °C Anal. calcd (%) for $C_{38}H_{42}N_4O_2S$: C, 73.75; H, 6.84; N, 9.05; found: C, 73.83; H, 6.90; N, 9.02.

Acknowledgements

We are grateful to the National Natural Science Foundation of China (no. 11104284 and no. 61101054) for the financial support.

Notes and references

1 J. Y. Lee, H. B. Bang, T. S. Kang and E. J. Park, *Eur. Polym. J.*, 2004, **40**, 1815–1822.

2 B. J. Coe, S. P. Foxon, E. C. Harper, M. Helliwell, J. Raftery, C. A. Swanson, B. S. Brunschwig, K. Clays, E. Franz, J. Garin, J. Orduna, P. N. Horton and M. B. Hursthouse, *J. Am. Chem. Soc.*, 2010, **132**, 1706–1723.
3 I. Fuks-Janczarek, J. M. Nunzi, B. Sahraoui, I. V. Kityk, J. Berdowski, A. M. Caminade, J. P. Majoral, A. C. Martineau, P. Frere and J. Roncali, *Opt. Commun.*, 2002, **209**, 461–466.
4 H. Y. Li and F. Jakle, *Macromol. Rapid Commun.*, 2010, **31**, 915–920.
5 K. H. Park, J. T. Lim, S. Song, Y. S. Lee, C. J. Lee and N. Kim, *React. Funct. Polym.*, 1999, **40**, 177–184.
6 S. W. Wang, L. S. Zhao, X. L. Zhang, X. Zhang, Z. S. Shi, Z. C. Cui, X. Chen and Y. Q. Yang, *Polym. Int.*, 2009, **58**, 933–938.
7 X. H. Zhou, J. Davies, S. Huang, J. D. Luo, Z. W. Shi, B. Polishak, Y. J. Cheng, T. D. Kim, L. Johnson and A. Jen, *J. Mater. Chem.*, 2011, **21**, 4437–4444.
8 F. Dumur, C. R. Mayer, E. Dumas, F. Miomandre, M. Frigoli and F. Secheresse, *Org. Lett.*, 2008, **10**, 321–324.
9 R. M. El-Shishtawy, F. Borbone, Z. M. Al-Amshany, A. Tuzi, A. Barsella, A. M. Asiri and A. Roviello, *Dyes Pigm.*, 2013, **96**, 45–51.
10 D. Briers, L. De Cremer, G. Koeckelberghs, S. Foerier, T. Verbiest and C. Samyn, *Macromol. Rapid Commun.*, 2007, **28**, 942–947.
11 J. M. Raimundo, P. Blanchard, P. Frere, N. Mercier, I. Ledoux-Rak, R. Hierle and J. Roncali, *Tetrahedron Lett.*, 2001, **42**, 1507–1510.
12 S. R. Hammond, O. Clot, K. A. Firestone, D. H. Bale, D. Lao, M. Haller, G. D. Phelan, B. Carlson, A. K. Y. Jen, P. J. Reid and L. R. Dalton, *Chem. Mater.*, 2008, **20**, 3425–3434.
13 Y. Q. Zhang, J. Ortega, U. Baumeister, C. L. Folcia, G. Sanz-Enguita, C. Walker, S. Rodriguez-Conde, J. Etxebarria, M. J. O'Callaghan and K. More, *J. Am. Chem. Soc.*, 2012, **134**, 16298–16306.
14 J. D. Luo, S. Huang, Y. J. Cheng, T. D. Kim, Z. W. Shi, X. H. Zhou and A. K. Y. Jen, *Org. Lett.*, 2007, **9**, 4471–4474.
15 Y. J. Cheng, J. D. Luo, S. Huang, X. H. Zhou, Z. W. Shi, T. D. Kim, D. H. Bale, S. Takahashi, A. Yick, B. M. Polishak, S. H. Jang, L. R. Dalton, P. J. Reid, W. H. Steier and A. K. Y. Jen, *Chem. Mater.*, 2008, **20**, 5047–5054.
16 Q. Q. Li, C. G. Lu, J. Zhu, E. Fu, C. Zhong, S. Y. Li, Y. P. Cui, J. G. Qin and Z. Li, *J. Phys. Chem. B*, 2008, **112**, 4545–4551.
17 J. Y. Wu, J. L. Liu, T. T. Zhou, S. H. Bo, L. Qiu, Z. Zhen and X. H. Liu, *RSC Adv.*, 2012, **2**, 1416–1423.
18 X. H. Zhou, J. D. Luo, J. A. Davies, S. Huang and A. K. Y. Jen, *J. Mater. Chem.*, 2012, **22**, 16390–16398.
19 J. B. Wu, B. A. Wilson, D. W. Smith and S. O. Nielsen, *J. Mater. Chem. C*, 2014, **2**, 2591–2599.
20 P. A. Sullivan and L. R. Dalton, *Acc. Chem. Res.*, 2010, **43**, 10–18.
21 C. Zhang, L. R. Dalton, M. C. Oh, H. Zhang and W. H. Steier, *Chem. Mater.*, 2001, **13**, 3043–3050.
22 X. Q. Piao, X. M. Zhang, S. Inoue, S. Yokoyama, I. Aoki, H. Miki, A. Otomo and H. Tazawa, *Org. Electron.*, 2011, **12**, 1093–1097.
23 J. A. Davies, A. Elangovan, P. A. Sullivan, B. C. Olbricht, D. H. Bale, T. R. Ewy, C. M. Isborn, B. E. Eichinger, B. H. Robinson, P. J. Reid, X. Li and L. R. Dalton, *J. Am. Chem. Soc.*, 2008, **130**, 10565–10575.
24 X. H. Ma, F. Ma, Z. H. Zhao, N. H. Song and J. P. Zhang, *J. Mater. Chem.*, 2010, **20**, 2369–2380.
25 C. Lee and R. G. Parr, *Phys. Rev. A*, 1990, **42**, 193–200.
26 C. M. Isborn, A. Leclercq, F. D. Vila, L. R. Dalton, J. L. Bredas, B. E. Eichinger and B. H. Robinson, *J. Phys. Chem. A*, 2007, **111**, 1319–1327.
27 L. T. Cheng, W. Tam, S. H. Stevenson, G. R. Meredith, G. Rikken and S. R. Marder, *J. Phys. Chem.*, 1991, **95**, 10631–10643.
28 L. T. Cheng, W. Tam, S. R. Marder, A. E. Stiegman, G. Rikken and C. W. Spangler, *J. Phys. Chem.*, 1991, **95**, 10643–10652.
29 P. R. Varanasi, A. K. Y. Jen, J. Chandrasekhar, I. N. N. Namboothiri and A. Rathna, *J. Am. Chem. Soc.*, 1996, **118**, 12443–12448.
30 M. M. M. Raposo, A. Sousa, G. Kirsch, P. Cardoso, M. Belsley, E. D. Gomes and A. M. C. Fonseca, *Org. Lett.*, 2006, **8**, 3681–3684.
31 L. R. Dalton, P. A. Sullivan and D. H. Bale, *Chem. Rev.*, 2010, **110**, 25–55.
32 I. Liakatas, C. Cai, M. Bosch, M. Jager, C. Bosshard, P. Gunter, C. Zhang and L. R. Dalton, *Appl. Phys. Lett.*, 2000, **76**, 1368–1370.
33 M. Thelakkat and H. W. Schmidt, *Adv. Mater.*, 1998, **10**, 219–223.
34 R. M. Ma, P. Guo, L. L. Yang, L. S. Guo, X. X. Zhang, M. K. Nazeeruddin and M. Gratzel, *J. Phys. Chem. A*, 2010, **114**, 1973–1979.
35 H. J. Xu, M. L. Zhang, A. R. Zhang, G. W. Deng, P. Si, H. Y. Huang, C. C. Peng, M. K. Fu, J. L. Liu, L. Qiu, Z. Zhen, S. H. Bo and X. H. Liu, *Dyes Pigm.*, 2014, **102**, 142–149.
36 R. V. Solomon, P. Veerapandian, S. A. Vedha and P. Venuvanalingam, *J. Phys. Chem. A*, 2012, **116**, 4667–4677.
37 L. R. Dalton, P. A. Sullivan, D. H. Bale and B. C. Olbricht, *Solid-State Electron.*, 2007, **51**, 1263–1277.
38 J. Wu, C. Peng, H. Xiao, S. Bo, L. Qiu, Z. Zhen and X. Liu, *Dyes Pigm.*, 2014, **104**, 15–23.
39 C. C. Teng and H. T. Man, *Appl. Phys. Lett.*, 1990, **56**, 1734–1736.
40 D. H. Park, C. H. Lee and W. N. Herman, *Opt. Express*, 2006, **14**, 8866–8884.
41 M. A. Mortazavi, A. Knoesen, S. T. Kowel, B. G. Higgins and A. Dienes, *J. Opt. Soc. Am. B*, 1989, **6**, 733–741.
42 H. Y. Huang, G. W. Deng, J. L. Liu, J. Y. Wu, P. Si, H. J. Xu, S. H. Bo, L. Qiu, Z. Zhen and X. H. Liu, *Dyes Pigm.*, 2013, **99**, 753–758.

43 Q. Q. Li, L. L. Lu, C. Zhong, J. Shi, Q. Huang, X. B. Jin, T. Y. Peng, J. G. Qin and Z. Li, *J. Phys. Chem. B*, 2009, **113**, 14588–14595.
44 O. P. Kwon, M. Jazbinsek, J.-I. Seo, P.-J. Kim, E.-Y. Choi, Y. S. Lee and P. Guenter, *Dyes Pigm.*, 2010, **85**, 162–170.
45 M. Q. He, T. M. Leslie and J. A. Sinicropi, *Chem. Mater.*, 2002, **14**, 2393–2400.
46 J. M. Raimundo, P. Blanchard, N. Gallego-Planas, N. Mercier, I. Ledoux-Rak, R. Hierle and J. Roncali, *J. Org. Chem.*, 2002, **67**, 205–218.